Engineered Redox-Responsive PEG Detachment Mechanism in PEGylated Nano-Graphene Oxide for Intracellular Drug Delivery

Huiyun Wen, Chunyan Dong, Haiqing Dong, Aijun Shen, Wenjuan Xia, Xiaojun Cai, Yanyan Song, Xuequan Li, Yongyong Li,* and Donglu Shi*

In biomedical applications, polyethylene glycol (PEG) functionalization has been a major approach to modify nanocarriers such as nano-graphene oxide for particular biological requirements. However, incorporation of a PEG shell poses a significant diffusion barrier that adversely affects the release of the loaded drugs. This study addresses this critical issue by employing a redox-responsive PEG detachment mechanism. A PEGylated nano-graphene oxide (NGO-SS-mPEG) with redox-responsive detachable PEG shell is developed that can rapidly release an encapsulated payload at tumor-relevant glutathione (GSH) levels. The PEG shell grafted onto NGO sheets gives the nanocomposite high physiological solubility and stability in circulation. It can selectively detach from NGO upon intracellular GSH stimulation. The surface-engineered structures are shown to accelerate the release of doxorubicin hydrochloride (DXR) from NGO-SS-mPEG 1.55 times faster than in the absence of GSH. Confocal microscopy shows clear evidence of NGO-SS-mPEG endocytosis in HeLa cells, mainly accumulated in cytoplasm. Furthermore, upon internalization of DXR-loaded NGO with a disulfide-linked PEG shell into HeLa cells, DXR is effectively released in the presence of an elevated GSH reducing environment, as observed in confocal microscopy and flow cytometric experiments. Importantly, inhibition of cell proliferation is directly correlated with increased intracellular GSH concentrations due to rapid DXR release.

H. Y. Wen, H. Q. Dong, A. J. Shen, W. J. Xia, X. J. Cai, Y. Y. Song, X. Q. Li, Dr. Y. Y. Li, Prof. D. L. Shi
The Institute for Advanced Materials and Nano Biomedicine
Tongji University School of Medicine
Shanghai 200092, P.R. China
E-mail: yongyong_li@tongji.edu.cn

Dr. C. Y. Dong
Department of Oncology
Shanghai East Hospital
Tongji University
Shanghai 200120, P.R. China

Prof. D. L. Shi
School of Electronic and Computing Systems
University of Cincinnati
Cincinnati, OH 45221, USA
E-mail: shid@ucmail.uc.edu

1. Introduction

There have been extensive research activities on graphene because of its unique physical and chemical properties.[1] Graphene and its derivative graphene oxide (GO) have shown important potential in biotechnology applications,[2] particularly in DNA detection,[3] cellular probing,[4] gene therapy,[5] photodynamic therapy,[6] and drug delivery.[7] In drug delivery, the integrity of graphene has to be maintained for its stability in physiological environments.[8] However, aggregation of functionalized GO has been found to be severe in physiological environments due to screening of electrostatic charges and nonspecific binding of proteins.[7] It is, therefore, important to address these critical issues on surface functionalization, stability, and biocompatibility for effective drug delivery.

Conjugation with hydrophilic coatings (e.g., PEGylation (PEG=polyethylene glycol),[7] poly(vinyl alcohol),[9] sulfonic acid groups[10]) has been previously explored by chemical modifications, and covalent or noncovalent strategies.[11] Among these methods, PEG functionalization has been known to prolong the circulation time of the pharmaceuticals in blood and avoid rapid uptake by macrophages of the mononuclear phagocyte system (MPS). As a result, high drug accumulation at tumor sites is attained through the enhanced permeability and retention (EPR) effect.[12] Dai et al. introduced a PEGylated nanoscale graphene oxide (NGO) for drug delivery with significantly improved stability in physiological solutions including serum.[7] Further in vivo behaviors of PEGylated NGO in mice were investigated by Liu et al. using a fluorescence labeling method.[13] Their results indicated that the impact of NGO was highly dependent on its surface PEG coating.

However, the benefit of the PEG coating is limited by its diffusion barrier, which adversely affects the drug release.[14] For effective therapy, rapid intracellular drug release is highly preferred upon immediate arrival of the delivery system. Therefore, a triggering mechanism can be identified such that shedding of a stabilizing PEG-coated NGO can respond to a specific stimulus, such as a reduction environment on the tumor site, to release the loaded drug. As is well known, the cellular redox environment in vivo is regulated by glutathione (GSH).[15] There is a significant GSH concentration difference between the exterior (2 μM) and interior (10 mM) of the cells. The cytosolic GSH level in some tumor cells has been found to be at least fourfold higher compared with normal cells.[16] This sharp contrast in GSH concentration may serve as an ideal stimulus for a PEG release mechanism.[17]

In this study, a unique NGO design was developed for intracellular drug delivery. The system is composed of NGO with a sheddable PEG shell attached via a disulfide linkage (NGO-SS-mPEG; mPEG = methoxy polyethylene glycol) that can respond to GSH changes for intracellular drug delivery. Several important design aspects include: a) modification of NGO stabilized with PEG conjugation for improved circulation and stability in physiological environments; b) drug loading of NGO via π–π stacking and hydrophobic interaction; and c) disulfide bond conjugated NGO that is prone to rapid cleavage through exchange reaction of thiol ligands by cellular GSH.

Figure 1 schematically illustrates the underlying mechanism of NGO design. In the presence of tumor-relevant GSH, NGO-SS-mPEG is internalized via endocytosis thereby initiating rapid disulfide cleavage of a stabilizing PEG shell, thus triggering efficient and controlled release of encapsulated drug payload. The engineered delivery system depicted in Figure 1 is able to address the critical issues of stability and circulation time, which enables rapid GSH-mediated drug release for tumor therapy. The intracellular release of doxorubicin hydrochloride (DXR) was studied with HeLa cells by using confocal laser scanning microscopy (CLSM) and flow cytometric analyses (fluorescence-activated cell sorting, FACS).

2. Results and Discussion

2.1. Preparation and Characterization of NGO-SS-mPEG

NGO was prepared by oxidizing flake graphite according to a modified Hummer's method.[18] The resulting NGO was dispersible in water but experienced fast aggregation in phosphate-buffered saline (PBS) and cell medium. Previously, Dai et al. concluded that this behavior was associated with screening of the electrostatic charges and nonspecific binding of proteins on NGO.[7] In this study, PEG functionalization of NGO was employed to disperse NGO with high physiological stability. However, PEG functionalization was found to be a significant diffusion barrier impeding the drug release. To address this problem, PEGylation of the NGO nanocarrier was developed by conjugating amino-terminated PEG to carboxylated NGO sheets via a disulfide bond. The unique design not only ensures high stability of NGO-SS-mPEG in physiological solution, but also facilitates the release of the encapsulated payload triggered by tumor-relevant GSH.

Figure 2 shows the synthetic route for the preparation of NGO-SS-mPEG nanocomposite. NGO-COOH is initially obtained by activating NGO with chloroacetic acid under strong basic conditions to convert the hydroxyl, epoxide, and ester groups into carboxylic acid (COOH) moieties. The intermediate product NGO-COOH increases the water solubility and more carboxylic acid groups are available for subsequent PEGylation. Amino-terminated PEG bearing a disulfide bond (mPEG-SS-NH$_2$) is then synthesized by reacting the succinate-activated mPEG-COOH with cystamine. Upon conjugating amino-terminated PEG with NGO-COOH, the final NGO-SS-mEPG exhibits high solubility and stability in PBS and cell medium, which is critical for biological applications.

Evaluation of a representative ^{1}H NMR spectrum obtained for NGO-SS-mPEG in D$_2$O (Supporting Information, Figure S1) shows characteristic chemical shifts of hydrogen atoms at the mPEG moiety ($\delta = 3.52$ ppm), indicating PEGylation of NGO. It should be noted that the reactive hydrogen on
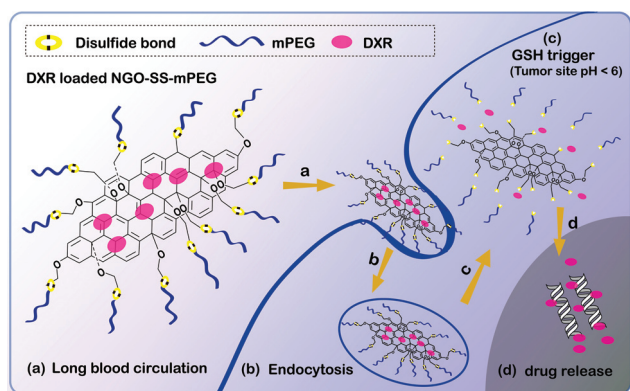

Figure 1. Schematic diagram showing antitumor activity of redox-sensitive DXR-loaded NGO-SS-mPEG: a) PEG-shielded NGO with disulfide linkage for prolonged blood circulation; b) endocytosis of NGO-SS-mPEG in tumor cells via the EPR effect; c) GSH trigger (GSH > fourfold relative to normal cells)[16] resulting in PEG detachment; and d) rapid drug release on the tumor site.
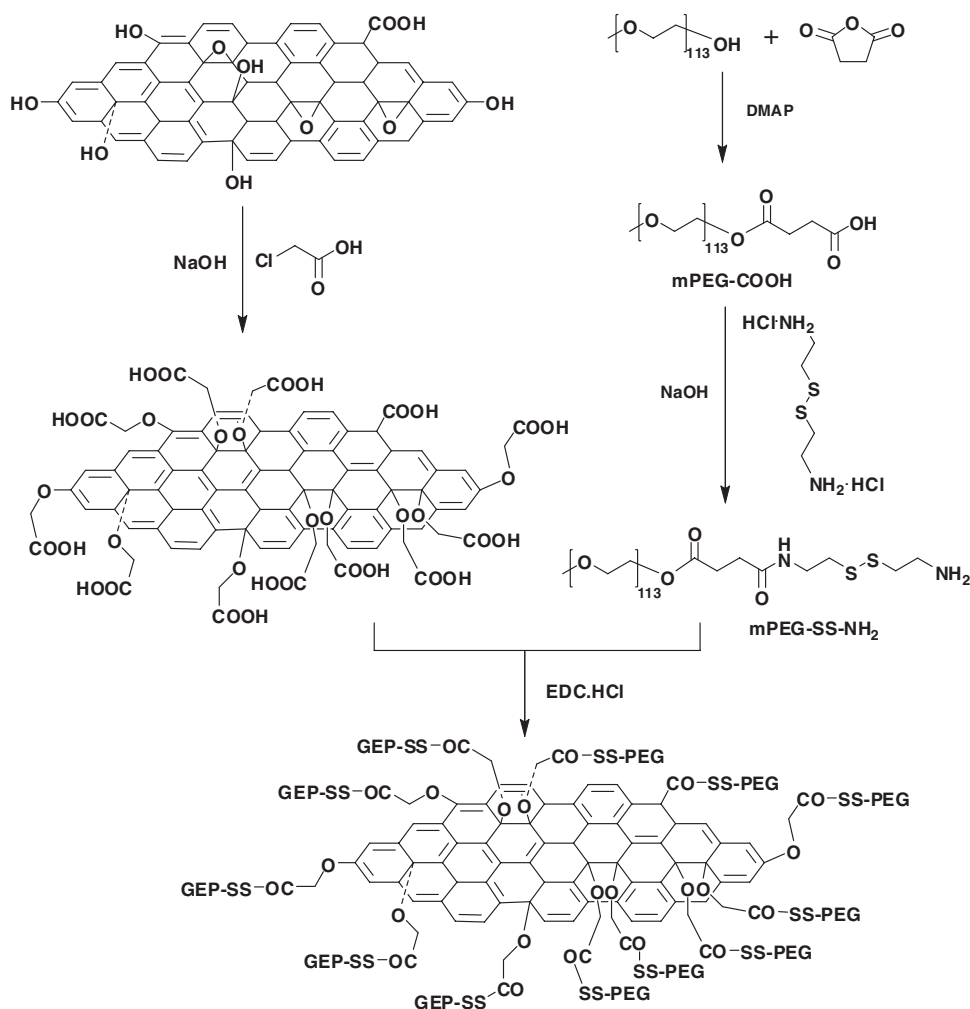
Figure 2. Synthesis pathway of disulfide-linked NGO-SS-mPEG. See the Experimental Section for details.

NGO makes it undetected in D$_2$O. Further evidence of PEG coating on NGO is confirmed by the FTIR spectra. As shown in the Supporting Information (Figure S2), a strong absorption band at 3403 cm^{-1} corresponds to the H−O stretching of NGO. The spectrum of NGO also exhibits the presence of C=O (ν_{C-O} at 1723 cm^{-1}), C=C ($\nu_{C=C}$ at 1619 cm^{-1}), and C−O (ν_{C-O} at 1060 cm^{-1}). However, with chemically bonded PEG on NGO, a characteristic band emerges at 1627 cm^{-1} corresponding to the amide carbonyl bond (O=CNH), which suggests the conjugation of PEG moieties on NGO sheets. Moreover, two peaks at 2880 and 1096 cm^{-1} are strong C−H vibrations and C−O−C bonds on PEG chains, respectively.

Atomic force microscopy (AFM) and transmission electron microscopy (TEM) were used to study the morphological characteristics of NGO and NGO-SS-mPEG. From the AFM image (**Figure 3**a), NGO shows a height of about 0.87 nm, which suggests a single-layer graphene sheet. However, an increase in sheet thickness is observed in NGO-SS-mPEG, mainly due to the attachment of PEG on both planes of the NGO sheet (Figure 3b). Most importantly, the resultant NGO-SS-mPEG remains well dispersed, which is critical for biological applications. TEM experimental results show
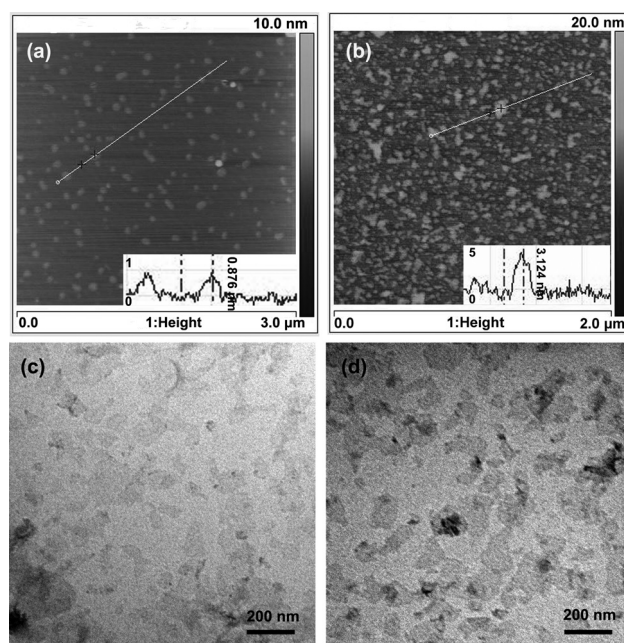

Figure 3. AFM images of a) NGO and b) NGO-SS-mPEG. TEM images of c) NGO-COOH, and d) NGO-SS-mPEG.
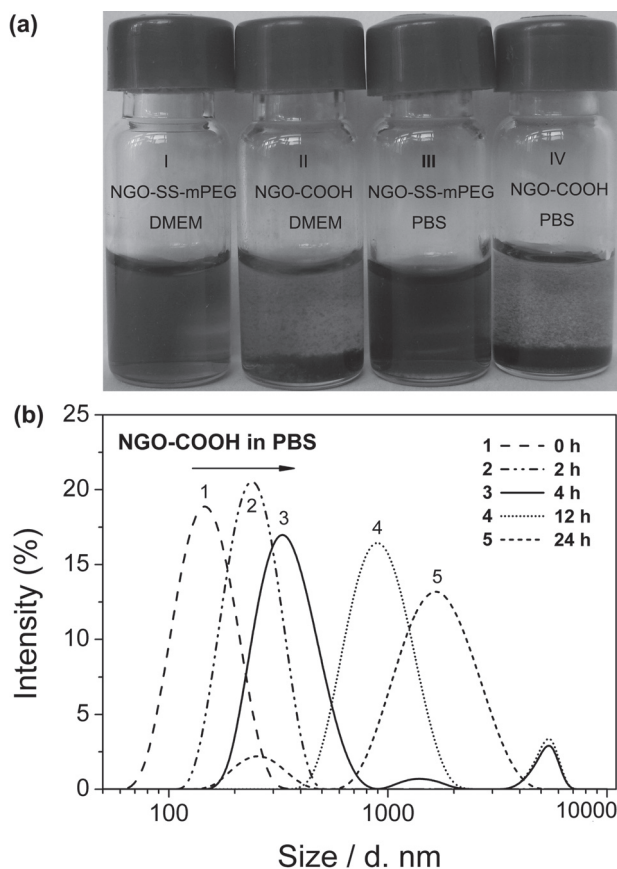
(a)

(b)

Figure 4. a) NGO-COOH and NGO-SS-mPEG dispersed in cell medium and PBS. NGO-COOH agglomerates in PBS and cell medium (II, IV). In sharp contrast, NGO-SS-mPEG remains stable in all solutions (I, III). b) Size–time dependence of NGO-COOH in 0.1 mM PBS as determined by dynamic light scattering (DLS).

that the lateral size of the NGO sheet (less than 200 nm) remains unchanged before and after PEG functionalization (Figure 3c,d).

2.2. Stability and GSH-Induced Size Change of NGO-SS-mPEG in Physiological Solution

As shown in **Figure 4**a, NGO-SS-mPEG exhibits high solubility and stability in both PBS and cell medium (Dulbecco's modified Eagle's medium, DMEM). In contrast, NGO-COOH experiences fast aggregation in PBS or cell medium. Aggregation of NGO-COOH in 0.1 mM PBS is observed by tracing the size alterations as a function of time. Upon exposure to 0.1 mM PBS, the average diameter of NGO-COOH significantly increases from 146 to 329 nm in a time interval of 4 h (Figure 4b). Formation of larger aggregates (>1000 nm) is even more pronounced at 12 h. In contrast, the average NGO-SS-mPEG size remains constant in water and 0.1 mM PBS (**Figure 5**a,b), thus indicating high stability in physiological solution.

In the design of the NGO nanocomposite, a disulfide bond (−S−S−) is introduced between grafted PEG and NGO moieties. This structure is relatively stable in plasma but can

be quickly cleaved by reducing agents such as GSH on the tumor site. The structural change of the nanocomposite is expected after PEG cleavage from NGO. The GSH-induced size changes of NGO-COOH and NGO-SS-mPEG are evident (Figure 4 and 5) when dispersed in deionized water and 0.1 mM PBS, respectively. In the presence of the biological reducing agent, the average diameter of NGO-SS-mPEG in deionized water decreases from 220 to 140 nm within 30 min, as a result of PEG shell detachment (Figure 5c). However, in 0.1 mM PBS with 10 mM GSH, the size of NGO-SS-mPEG significantly increases after 10 min from 220 to 776 nm (Figure 5d). Precipitation is found to be even more severe after 30 min due to the instability of NGO in PBS. These experimental results indicate the detachment of PEG coating from the planes of the NGO-SS-mPEG sheet.

2.3. Drug Loading and GSH-Induced in vitro DXR Release

Driven by noncovalent interaction including π–π stacking and hydrophobic interactions, the cytotoxic anticancer agent DXR has been reported to be loaded onto NGO in a very efficient way.[19] DXR was mixed with NGO-SS-mPEG in water solution by sonication. The UV/Vis spectrum of the resultant solution shows an absorption peak at 490 nm, which indicates successful loading of DXR onto NGO-SS-mPEG (Supporting Information, Figure S3). The loading process results in fluorescence quenching of DXR (**Figure 6**a) due to the photoinduced electron-transfer effect.[20] Interestingly, fluorescence could be recovered by addition of ethanol. This phenomenon was reported to be associated with desorption of DXR from NGO-SS-mPEG.[5,21] The presence of ethanol is destructive to noncovalent interaction between DXR and NGO-SS-mPEG, thus leading to the fluorescence recovery.

The in vitro release of DXR can be well observed via the fluorescence signals of DXR. The release behavior of DXR from NGO-SS-mPEG was studied by fluorescence spectroscopy. A 10% DXR to NGO-SS-mPEG ratio was set for a given pH value at different GSH concentrations. As shown in Figure 6b, for a pH of 5.5 without GSH, less than 35% DXR is released in a time period of 48 h. It should be noted that the above environment is physiologically simulated to the tumor pH value and extracellular GSH concentrations (e.g., plasma).[22] However, upon exposure to 10 mM GSH, a typical level in tumor cells (i.e., cytosol, cell), 55% DXR is released in 48 h at the same pH, thereby indicating an accelerated process. In control experiments performed at pH 7.4 without GSH, which corresponds to the physiological pH, only less than 5% of the anticancer agent is released in a period of 72 h. Drug release acceleration is again observed for an addition of 10 mM GSH at the same pH value.

In addition to the GSH-induced drug release, the drug release from NGO-SS-mPEG is much faster at pH 5.5 (Figure 6b). However, the pH-controlled release relies on the protonation effect of DXR at low pH, which could make DXR more hydrophilic and water soluble, thus leading to the increased release of DXR in aqueous solution. Similar pH-responsive drug release behavior was observed previously for NGO and PEGylated NGO.[20,21]
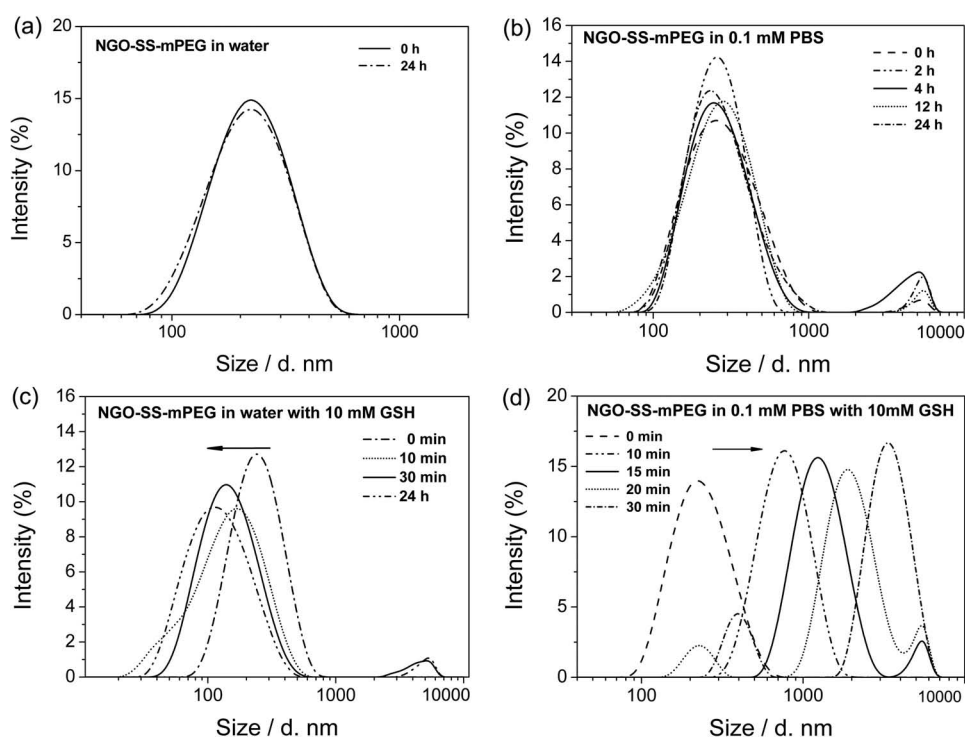
Figure 5. Size–time dependences of NGO-SS-mPEG when dispersed in water or PBS, with or without GSH as determined by DLS. NGO-SS-mPEG is stable in both water (a) and 0.1 mM PBS (b); the size of NGO-SS-mPEG decreases in water with 10 mM GSH (c), and NGO-SS-mPEG aggregates in 0.1 mM PBS with 10 mM GSH (d). The aggregation is mainly due to detachment of the PEG shell from the planes of the NGO sheets.

In this study we mainly focus on redox triggering release. The drug release acceleration behavior upon redox triggering is most likely associated with detachment of the PEG diffusion barrier on both planes of the NGO sheet. The release data showed a difference between samples treated with or without redox trigger, although it is not as pronounced as in the situation with either the size change upon redox trigger (Figure 5) or pH triggering drug release (Figure 6b). This behavior can be attributed to size aggregation induced by GSH addition, which is not favorable for drug diffusion. However, the aggregation is expected to be greatly reduced due to non free diffusion and low concentration of NGO in the in vitro and in vivo applications.

2.4. Redox-Dependent Biological Efficacy of DXR-Loaded NGO-SS-mPEG

To assess the therapeutic efficacy of DXR loading, it is critical to study the cellular uptake of NGO-SS-mPEG. Fluorescence spectra in the visible range show that NGO-SS-mPEG has a rather broad emission from 450 to 700 nm, with a peak at ≈520 nm, excited at 405 nm (**Figure 7**a). As the incubation time increases from 1 to 6 h, the NGO-SS-mPEG fluorescence intensifies (Figure 7b), clearly indicating endocytosis of NGO-SS-mPEG in tumor cells. Flow cytometric analysis shows that the intracellular concentration of NGO-SS-mPEG increases after incubation with HeLa cells for 2 h in comparison with the control (Figure 7c).

Further evaluation of the therapeutic efficacy of DXR-loaded NGO-SS-mPEG was carried out in vitro by quantifying the cell viability of HeLa cells using the WST-1 assay. As shown in **Figure 8**a, NGO-SS-mPEG without DXR does not significantly affect proliferation of the cell line up to a concentration of 1 mg mL^{-1}. However, either free DXR or DXR-loaded NGO-SS-mPEG has effectively reduced the viability of HeLa cells in a dose-dependent fashion (Figure 8a). The maximum efficacy of ≈90% growth inhibition after 24 h is achieved at the concentrations of equivalent DXR dose >20 mg L^{-1}.

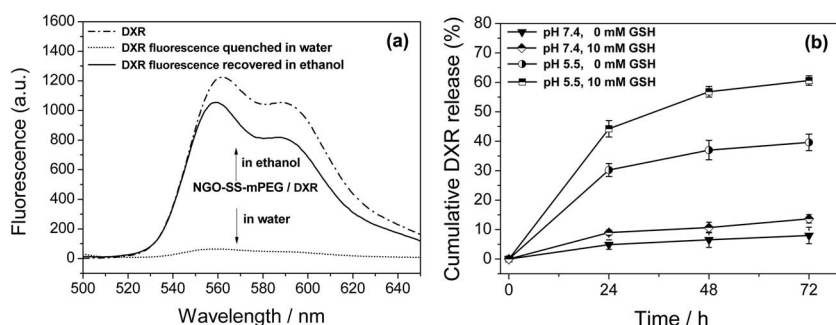The study on GSH-mediated drug release was carried out in HeLa cells

Figure 6. a) Fluorescence spectra of DXR and DXR-loaded NGO-SS-mPEG in water at 470 nm excitation wavelength. Significant fluorescence quenching is observed for DXR-loaded NGO-SS-mPEG and fluorescence is recovered by addition of ethanol. b) GSH-mediated drug release from DXR-loaded NGO-SS-mPEG at pH 7.4 and 5.5.
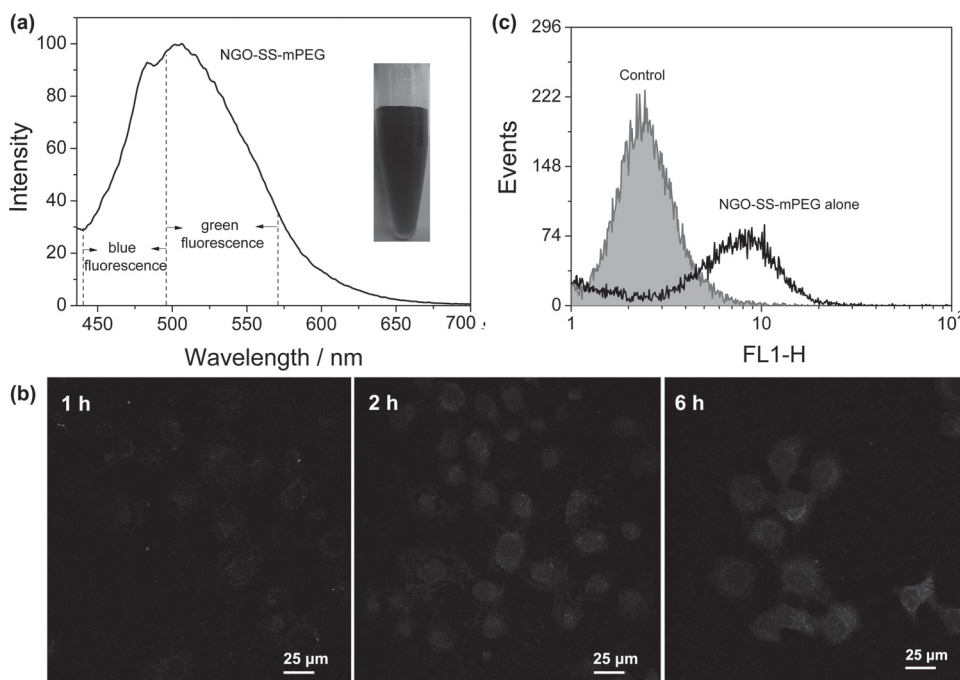
© 2012 Wiley-VCH Verlag GmbH & Co. KGaA, Weinheim

Figure 7. a) Fluorescence spectra of NGO-SS-mPEG in the visible range under an excitation of 405 nm and an optical image of NGO-SS-mPEG in aqueous solution (inset). b) Cellular uptake of NGO-SS-mPEG for 6 h by CLSM under an excitation of 405 nm. c) Flow cytometric analyses of HeLa cells incubated with NGO-SS-mPEG for 2 h. HeLa cells without NGO-SS-mPEG treatment are used as the control. Fluorescence intensity is denoted as FL1-H.

in terms of GSH concentration and tumor cell viability. The intracellular GSH concentration was controlled by using GSH-reduced ethyl ester (GSH-OEt) as an external enhancer of the cellular GSH level.[22] Previous research indicated that GSH-OEt had no cytotoxicity and penetrated cellular membranes to generate GSH with rapid hydrolysis in cytoplasm.[23] In the drug release study, HeLa cells in culture media were pretreated with 0 or 10 mM GSH-OEt for 2 h. For DXR-loaded NGO-SS-mPEG, it should be noted that at higher DXR concentrations, the passive uptake is high so that tumor cells are killed with or without the presence of GSH. However, a minimal DXR concentration is required for a noticeable biological effect. Based on the results of in vitro

cell cytotoxicity tests, the cells were further incubated for 6 or 24 h with various concentrations of DXR-loaded NGO-SS-mPEG (0.25, 0.125, or 0.0625 mg mL^{-1}). The equivalent DXR doses are 23.3, 11.6, and 5.8 mg L^{-1}, respectively (Figure 8b). As expected, GSH-OEt addition to cell culture media potentiates the inhibitory effect of DXR-loaded NGO-SS-mPEG, especially at the concentrations of 0.25 and 0.125 mg mL^{-1} for 6 and 24 h of incubation, respectively.

CLSM results of HeLa cells treated with DXR-loaded NGO-SS-mPEG (0.25 mg mL^{-1}) clearly indicate the acceleration of intracellular DXR release at different GSH levels (**Figure 9**). As shown in Figure 9a, stronger DXR fluorescence is observed in both cytoplasm and nucleus of GSH-OEt pretreated HeLa cells, especially in the nucleus. It is critical for DXR to be released from NGO-SS-mPEG and accumulate in the nucleus for anticancer activity via interaction with DNA.[24] Consistent with the results of CLSM, flow cytometric analyses show that incubating with DXR-loaded NGO-SS-mPEG (0.25, 0.125, 0.0625 mg mL^{-1}) for 2 h results in significant DXR fluorescence difference between the 0 and 10 mM GSH-OEt pretreated HeLa cells, thus indicating enhanced DXR release (**Figure 10**). It is noteworthy that pretreatment of HeLa cells with GSH-OEt upregulates the intracellular GSH concentration, and subsequently accelerates the DXR release from the NGO-SS-mPEG due to GSH-responsive disulfide linkage degradation between the
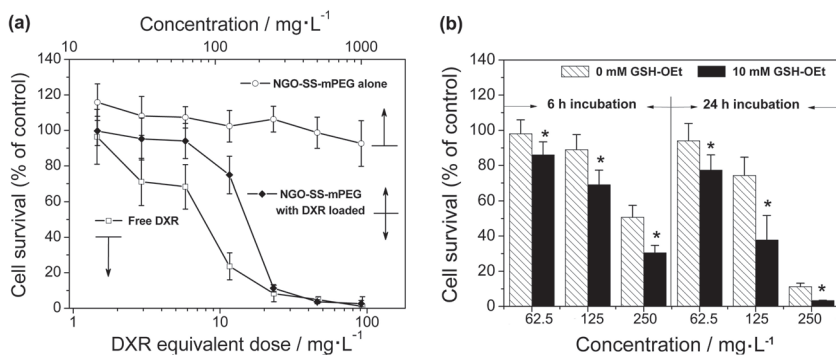

Figure 8. a) Cell proliferation of HeLa cells incubated with free DXR, NGO-SS-mPEG, and DXR-loaded NGO-SS-mPEG for 24 h. Data are presented as the mean ± standard deviation (SD; $n = 5$). b) Cell proliferation of pretreated HeLa cells with either 0 or 10 mM GSH-OEt incubated with DXR-loaded NGO-SS-mPEG (0.25, 0.125, 0.0625 mg mL^{-1}) for the time periods indicated. *$p < 0.05$ by Student's t-test.
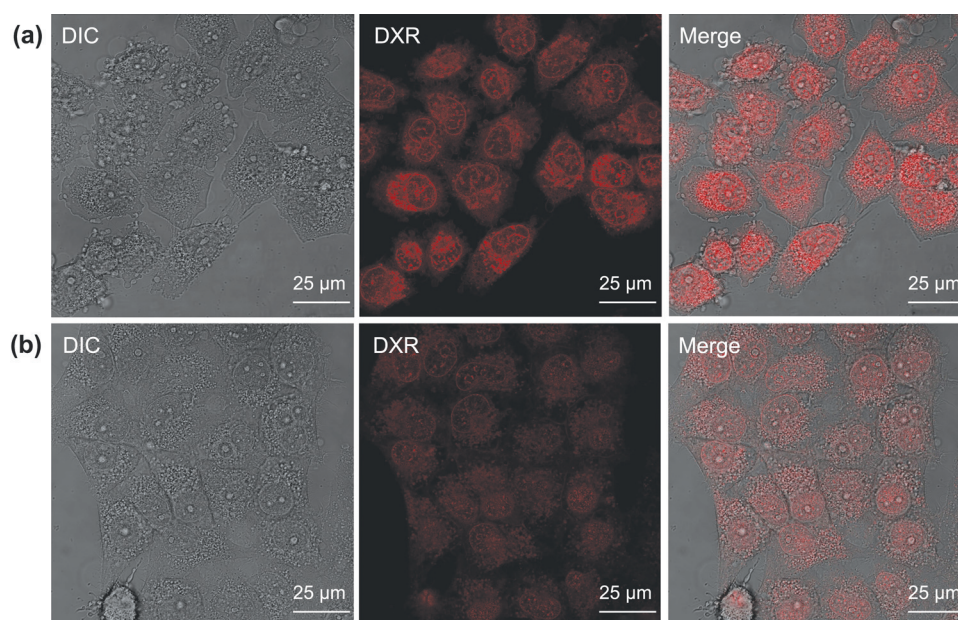
Figure 9. Representative CLSM images of a) 10 mM GSH-OEt and b) 0 mM GSH-OEt pretreated HeLa cells after 6 h of incubation with DXR-loaded NGO-SS-mPEG (0.25 mg mL^{-1}). The red channel visualizes DXR fluorescence.
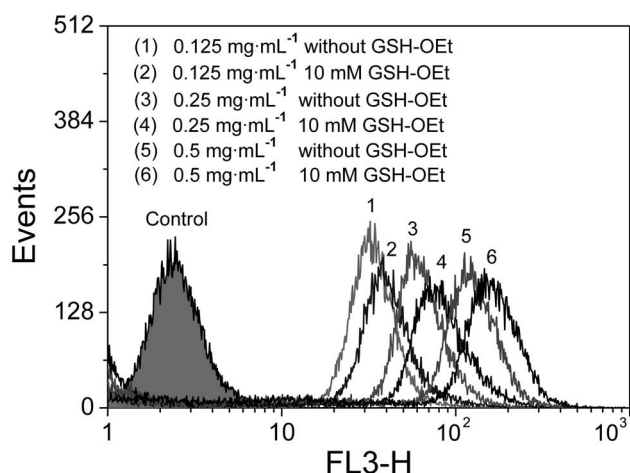

Figure 10. Flow cytometric analyses of nontreated and 10 mM GSH-OEt pretreated HeLa cells incubated with DXR-loaded NGO-SS-mPEG at the concentrations indicated for 2 h. The equivalent DXR dose is 46.5, 23.3, and 11.6 mg L^{-1}, respectively. HeLa cells without any treatment are used as control. Fluorescence intensity is denoted as FL3-H.

PEG and NGO sheets. Therefore, the enhanced intracellular DXR fluorescence in GSH-OEt pretreated cells is associated with the detachment of the PEG diffusion barrier from both planes of the NGO sheet. The experimental results show that GSH-triggered intracellular release is a dominant drug-release mechanism, responsible for antitumor activities of the DXR-loaded NGO-SS-mPEG composites.

3. Conclusion

Nano-graphene oxide composed of a sheddable PEG shell attached via a disulfide linkage (NGO-SS-mPEG) has been designed and developed for tumor-selective drug delivery.

Upon exposure to 10 mM GSH, reductive cleavage of the disulfide-linked PEG shell initiates rapid release of encapsulated payload. Cell proliferation assays have been performed with HeLa cells that demonstrate the pharmacological efficacy of DXR released from NGO-SS-mPEG in the presence of elevated GSH concentrations. Consequently, redox-sensitive NGO-SS-mPEG nanocarriers are able to preferentially deliver encapsulated drug to targeted tumor sites with high intracellular GSH concentrations. The specially engineered nanocarrier will address some of the critical issues on stability and circulation time and achieve drug delivery in a tumor-selective and controlled fashion. It will also provide many other approaches and alternatives in biomedical applications, such as photodynamic therapy and gene therapy.

4. Experimental Section

Materials: Native flake graphite was purchased from Shanghai Yifan Graphite Co. Ltd., with an average particle diameter of 25 μm (purity ≥99.9%). H$_2$SO$_4$ (98%), H$_2$O$_2$ (30 wt%), NaNO$_3$ (AR), KMnO$_4$ (AR), and chloroacetic acid (AR) were obtained from Shanghai Chemical Reagent Co. Ltd. Polyethylene glycol monomethyl ether (CH$_3$O-PEG, M_n: 5000) was purchased from GL Biochem Ltd. (Shanghai) and used as received. Cystamine dihydrochloride (98%), 1-ethyl-3-(3-dimethylaminopropyl) carbodiimide hydrochloride (EDC·HCl, 98.5%), N-hydroxysuccinimide (NHS, 98%), 4-dimethylaminopyridine (DMAP, 99%), glutathione (GSH, 98%), and succinic anhydride (AR) were purchased from Aladdin Chemistry Co. Ltd. (Shanghai) and used as received. Doxorubicin hydrochloride (DXR, Aldrich) was used as received. Glutathione reduced ethyl ester (GSH-OEt, ≥90%) was purchased from Sigma–Aldrich. 1,4-Dioxane, dichloromethane (DCM), and N,N-dimethylformamide (DMF) were purchased from Shanghai Chemical Reagent Co. Ltd., dried by

refluxing over CaH_2, and distilled or vacuum distilled before use. The dialysis tube (Spectra/Por 7, molecular weight cutoff, MWCO: 8000–10 000) was purchased from Spectrum Laboratories Inc. Dulbecco's modified Eagle's medium (DMEM), fetal bovine serum (FBS), penicillin–streptomycin, trypsin, and Dulbecco's phosphate-buffered saline (DPBS) were obtained from Gibco Invitrogen Corp. Paraformaldehyde (4%) was purchased from DingGuo Chang Sheng Biotech. Co. Ltd. WST-1 cell proliferation and cytotoxicity assay kits were purchased from Beyotime Institute of Biotechnology.

Synthesis of mPEG-COOH: Succinic anhydride (0.1 g, 1 mmol) and DMAP (0.05 g, 0.4 mmol) were added to a 1,4-dioxane (50 mL) solution of mPEG (M_n: 5000, 2 g, 0.4 mmol). The reaction mixture was stirred at room temperature (RT) for 24 h under nitrogen. After evaporation of the solvent under vacuum, saturated aqueous NaCl was added and the aqueous solution was extracted with DCM (3 × 20 mL). The organic extracts were combined and mPEG-COOH was isolated by precipitation from DCM to ethyl ether and was dried under vacuum. Yield: 86%.

Synthesis of mPEG-SS-NH₂: Cystamine dihydrochloride (0.17 g, 1.1 mmol) and NaOH (88 mg, 2.2 mmol) were stirred in water solution (30 mL) for 30 min at RT and distilled at 45 °C under vacuum to remove water. The DCM solution was then added to the mixture to dissolve the cystamine by filtering the salt. After distilling at 30 °C under vacuum to remove DCM, the cystamine was isolated. EDC·HCl (0.62 mmol) and NHS (0.23 mmol) were added to a DCM solution of mPEG-COOH (1 g, 0.2 mmol) and the mixture was stirred at RT for 5 h under nitrogen. The solution of cystamine (0.15 g, 1 mmol) in DCM prepared as described above was subsequently added dropwise to the above mixture for another 24 h of reaction at RT. Finally, the product mPEG-SS-NH₂ was isolated by precipitation from DCM to ethyl ether and was dried under vacuum. Yield: 79%.

Synthesis of PEGylated NGO with a Disulfide Linkage (NGO-SS-mPEG): NGO was prepared by the modified Hummers' method using natural flake graphite.[18b] To improve the stability of NGO in the cell culture medium, modification of NGO with PEG was carried out by formation of an amide bond between mPEG-SS-NH₂ and NGO in the presence of EDC. Briefly, carboxylic acid groups were first introduced to NGO by reaction with chloroacetic acid according to our previous work.[18a] EDC (10 mg) was then added to the NGO-COOH suspension (10 mL, 1 mg mL^{-1}) and the mixture was sonicated for 5 min. mPEG-SS-NH₂ (100 mg) was subsequently added to the above suspension and stirred for 24 h at RT. The final product (NGO-SS-mPEG) was obtained by dialysis of the mixture against distilled water to remove the excess reactant.

Characterization Methods: FTIR spectra of powdered samples were recorded on a Tensor 27 FTIR spectrometer (Bruker AXS, China). ^1H NMR spectra were acquired using an Avance 500 MHz spectrometer (Bruker BioSpin, Switzerland). Samples were dissolved in D_2O, and TMS was used as standard. UV/Vis detection and fluorescence spectra were obtained with an ultraviolet–visible spectrophotometer (Varian Ltd., Hong Kong) and a Hitachi F2500 luminescence spectrometer (Hitachi Ltd., Hong Kong), respectively. AFM images of samples deposited from a dilute aqueous dispersion (0.01 mg mL^{-1}) on a freshly cleaved silicon surface were observed in the tapping mode with an SPA-300HV instrument. TEM was carried out on a Hitachi H7100 transmission electron microscope (Hitachi Ltd., Hong Kong). Briefly, a

drop of sample suspension was placed on a copper grid fitted with a Formvar film and dried before measurement. Size distribution of NGO-SS-mPEG was determined by a Nano-ZS 90 Nanosizer (Malvern Instruments Ltd., Worcestershire, UK). The cellular uptake was observed using fluorescence microscopy (Nikon ECLIPSE 80i) and CLSM (Leica TCS SP5 II, Germany). Flow cytometric analysis was carried out with a FACS Calibur flow cytometer (BD Biosciences, USA).

GSH-Induced Size Change of NGO-SS-mPEG: The protocol used to assess the stability of PEGylated NGO in response to GSH was by DLS measurement. Typically, NGO-SS-mPEG was placed at 37 °C in PBS (0.1 mM) or deionized water after addition of sufficient GSH to achieve a 10 mM GSH reducing environment. At designated time intervals, NGO-SS-mPEG size distribution was determined by dynamic laser light scattering using the Nano-ZS 90 Nanosizer (Malvern Instruments Ltd., Worcestershire, UK).

Fabrication of DXR-Loaded NGO-SS-mPEG: Loading of doxorubicin hydrochloride (DXR) onto NGO-SS-mPEG was done by simply adding DXR (1 mL, 25 μg mL^{-1}) to the NGO-SS-mPEG aqueous suspension (5 mL, 0.05 mg mL^{-1}) at a given pH value. The suspension was sonicated for 0.5 h and then stirred for 24 h in the dark at RT. The dialysis of the product was exhausted against deionized water through a dialysis membrane (M_w: 10–12 kDa) to remove the unloaded DXR. DXR loading on NGO-SS-PEG was determined by UV/Vis spectrometry by the absorbance at 480–490 nm and by luminescence spectrometry (exc. = 470 nm, em. = 559 nm). The amount of DXR loaded on NGO-SS-mPEG was quantified by luminescence spectrometry according to a modified method reported by Chen et. al.[20]

GSH-Induced DXR in vitro Release: The release profiles of DXR were studied in release media of 0 or 10 mM GSH concentration at different pH values; the mixture was placed in a shaking bed at 37 °C with a speed of 150 rpm. At predetermined time intervals, the samples were centrifuged. The concentration of released DXR in the supernatant was determined based on the standard curve: C (μg mL^{-1}) = I/156.32, where I is the fluorescence intensity at excitation and emission wavelengths of 470 and 559 nm, respectively. The cumulative amount of DXR released from NGO-SS-mPEG over 72 h was calculated according to: Cumulative DXR release [%] = (M_t/M_0) × 100%, where M_t is the total amount of DXR released from NGO-SS-mPEG at time t, and M_0 is the amount of DXR initially loaded into the NGO-SS-mPEG.

Cell Lines: Human epitheloid cervix carcinoma (HeLa) cells were supplied by the Cell Center of the Tumor Hospital of Fudan University (Shanghai, China). Cells were propagated in T-75 flasks under an atmosphere of 5% CO_2 at 37 °C and grown in DMEM supplemented with 10% FBS and 0.1% penicillin–streptomycin.

In vitro Cytotoxicity of Free DXR, NGO-SS-mPEG, and DXR-Loaded NGO-SS-mPEG by WST-1 Assay: The cytotoxicities of free DXR, NGO-SS-mPEG, and DXR-loaded NGO-SS-mPEG against HeLa cells were determined by standard WST-1 assay using the WST-1 cell proliferation and cytotoxicity assay kit. In brief, HeLa cells were seeded in 96-well plates (5000 cells/well) using DMEM (200 μL) and incubated at 37 °C for 24 h. The medium in each well was then replaced with culture medium (150 μL) containing treatments of free DXR, NGO-SS-mPEG, or DXR-loaded NGO-SS-mPEG. The concentration of free DXR was diluted with culture medium to obtain a concentration range of 1.45–93 mg L^{-1}. The concentration of NGO-SS-mPEG and DXR-loaded NGO-SS-mPEG was diluted with

culture medium to obtain a concentration range of 15.6×10^{-3} to 1 mg mL^{-1}. After incubation for 24 h, the medium in each well was replaced with fresh medium (100 μL) and WST-1 solution (10 μL). The plate was incubated for a further 4 h at 37 °C, which allowed viable cells to reduce WST-1 into the orange formazan crystal. The plate was read at 450 nm on a Bio-Rad microplate reader (Thermo Fisher Scientific, Waltham, MA, USA).

The relative cell viability (%) was calculated by the following equation: Cell viability = (OD$_{treated}$/OD$_{control}$) × 100%, where OD$_{treated}$ (OD = optical density) was obtained by comparing the OD with that of control wells containing only cell culture medium. Data are presented as the average (SD, $n = 5$).

Redox-Dependent Intracellular DXR Delivery by WST-1: To estimate the change in intracellular DXR as a function of GSH, HeLa cells (seeded 5000 cells/well in a 96-well plate) were incubated for 24 h and then treated with cell culture media containing 0 or 10 mM GSH-OEt for another 2 h. Cells were washed with PBS and incubated at 37 °C for an additional 6 or 24 h with DXR-loaded NGO-SS-mPEG of different concentrations (150 μL; 0.5, 0.25, 0.125 mg mL^{-1}) in complete DMEM. Cells without GSH-OEt treatment were used as the control determined by WST-1 assay.

Cellular Uptake of NGO-SS-mPEG: To monitor the time-dependent cellular uptake of NGO-SS-mPEG, HeLa cells (1×10^5 cells/well) were incubated with NGO-SS-mPEG (0.5 mg mL^{-1}). At predetermined time intervals (1, 2, and 6 h) the culture medium was removed and cells were rinsed twice with DPBS, then paraformaldehyde (4%) was added and the mixture was kept at RT (15 min). The cells were rinsed twice again with DPBS, and imaged by CLSM (Leica TCS SP5 II, Germany).

Cellular uptake of NGO-SS-mPEG was also measured by flow cytometric analysis (FACS). Briefly, HeLa cells (1×10^5 cells/well) were seeded onto six-well plates and incubated for 24 h. Cells were incubated at 37 °C for an additional 2 h with NGO-SS-mPEG in complete DMEM. Cells were washed with DPBS twice and harvested, then suspended in paraformaldehyde (500 μL, 2%) for FACS analyses using a FACSCalibur flow cytometer (BD Biosciences, USA).

Redox-Dependent Intracellular Drug Release and Flow Cytometric Analysis (FACS) of DXR-Loaded NGO-SS-mPEG: The cellular uptake of DXR-loaded NGO-SS-mPEG and intracellular DXR release behavior were characterized by a similar method to that described above. Briefly, HeLa cells (1×10^5 cells/well) were incubated in six-well plates. After 24 h of incubation, the cells were treated with cell culture media containing 0 or 10 mM GSH-OEt for 2 h. The cells were washed with PBS and incubated at 37 °C for an additional 6 h with DXR-loaded NGO-SS-mPEG (2 mL, 0.25 mg mL^{-1}) in complete DMEM. The culture medium was removed and the cells were rinsed twice with DPBS, then 4% paraformaldehyde was added and the mixture was kept at RT for 15 min. The cells were rinsed twice again with DPBS, and observed by using CLSM (Leica TCS SP5 II, Germany).

For FACS analyses, HeLa cells (1×10^5 cells/well) were seeded onto six-well plates and incubated for 24 h. Cells were treated with or without GSH-OEt for 2 h, and washed with DPBS. Cells were then incubated at 37 °C for an additional 2 h with DXR-loaded NGO-SS-mPEG (0.5, 0.25, 0.125 mg mL^{-1}) in complete DMEM. The cells were washed with DPBS twice and harvested, then suspended in paraformaldehyde (500 μL, 2%) for FACS analyses using a FACS-Calibur flow cytometer (BD Biosciences, USA).

Statistical Analysis: In vitro cell proliferation assay was performed in five duplicate wells. Mean and standard deviations were tabulated. Student's *t*-test was used to determine the statistical difference among groups at a significance level $p < 0.05$. Data are presented as means ± standard errors.

Supporting Information

Supporting Information is available from the Wiley Online Library or from the author.

Acknowledgements

[1] a) K. S. Novoselov, A. K. Geim, S. V. Morozov, J. Y. Zhang, S. V. Dubonos, I. V. Grigorieva, A. A. Firsov, *Science* **2004**, *306*, 666; b) S. Stankovich, D. A. Dikin, G. H. B. Dommett, K. M. Kohlhaas, E. J. Zimney, E. A. Stach, R. D. Piner, S. T. Nguyen, R. S. Ruoff, *Nature* **2006**, *442*, 282; c) N. Xiao, X. C. Dong, L. Song, D. Y. Liu, Y. Y. Tay, S. X. Wu, L. J. Li, Y. Zhao, T. Yu, H. Zhang, W. Huang, H. H. Hng, P. M. Ajayan, Q. Y. Yan, *ACS Nano* **2011**, *5*, 2749; d) H. L. Wang, J. T. Robinson, G. Diankov, H. J. Dai, *J. Am. Chem. Soc.* **2010**, *132*, 3270; e) A. K. Geim, *Science* **2009**, *324*, 1530; f) X. Huang, Z. Y. Yin, S. X. Wu, X. Y. Qi, Q. Y. He, Q. C. Zhang, Q. Y. Yan, F. Boey, H. Zhang, *Small* **2011**, *7*, 1876; g) L. Z. Feng, Z. Liu, *Nanomedicine* **2011**, *6*, 317.
[2] Y. Wang, Z. Li, J. Wang, J. Li, Y. Lin, *Trends Biotechnol.* **2011**, *29*, 205.
[3] S. J. He, B. Song, D. Li, C. F. Zhu, W. P. Qi, Y. Q. Wen, L. H. Wang, S. P. Song, H. P. Fang, C. H. Fan, *Adv. Funct. Mater.* **2010**, *20*, 453.
[4] Y. Wang, Z. H. Li, D. H. Hu, C. T. Lin, J. H. Li, Y. H. Lin, *J. Am. Chem. Soc.* **2010**, *132*, 9274.
[5] L. M. Zhang, Z. X. Lu, Q. H. Zhao, J. Huang, H. Shen, Z. J. Zhang, *Small* **2011**, *7*, 460.
[6] B. Tian, C. Wang, S. Zhang, L. Z. Feng, Z. Liu, *ACS Nano* **2011**, *5*, 7000.
[7] Z. Liu, J. T. Robinson, X. M. Sun, H. J. Dai, *J. Am. Chem. Soc.* **2008**, *130*, 10876.
[8] D. Y. Cai, M. Song, *J. Mater. Chem.* **2010**, *20*, 7906.
[9] N. G. Sahoo, H. Q. Bao, Y. Z. Pan, M. Pal, M. Kakran, H. K. F. Cheng, L. Li, L. P. Tan, *Chem. Commun.* **2011**, *47*, 5235.
[10] Y. C. Si, E. T. Samulski, *Nano Lett.* **2008**, *8*, 1679.
[11] a) X. Y. Qi, K. Y. Pu, X. Z. Zhou, S. X. Wu, Q. L. Fan, B. Liu, F. Boey, W. Huang, H. Zhang, *Angew. Chem. Int. Ed.* **2010**, *49*, 9426; b) R. J. Xing, G. Liu, Q. M. Quan, A. Bhirde, G. F. Zhang, A. Jin, L. H. Bryant, A. Zhang, A. Liang, H. S. Eden, Y. L. Hou, X. Y. Chen, *Chem. Commun.* **2011**, *47*, 12152.
[12] a) G. Prencipe, S. M. Tabakman, K. Welsher, Z. Liu, A. P. Goodwin, L. Zhang, J. Henry, H. J. Dai, *J. Am. Chem. Soc.* **2009**, *131*, 4783; b) K. Riehemann, S. W. Schneider, T. A. Luger, B. Godin, M. Ferrari, H. Fuchs, *Angew. Chem., Int. Ed.* **2009**, *48*, 872.
[13] K. Yang, S. Zhang, G. X. Zhang, X. M. Sun, S. T. Lee, Z. Liu, *Nano Lett.* **2010**, *10*, 3318.
[14] a) B. Romberg, W. E. Hennink, G. Storm, *Pharm. Res.* **2008**, *25*, 55; b) S. D. Li, L. Huang, *J. Controlled Release* **2010**, *145*, 178;

c) H. Hatakeyama, H. Akita, H. Harashima, *Adv. Drug Delivery Rev.* **2011**, *63*, 152.

[15] N. Ballatori, S. M. Krance, S. Notenboom, S. Shi, K. Tieu, C. L. Hammond, *Biol. Chem.* **2009**, *390*, 191.

[16] F. H. Meng, W. E. Hennink, Z. Y. Zhong, *Biomaterials* **2009**, *30*, 2180.

[17] a) S. Takae, K. Miyata, M. Oba, T. Ishii, N. Nishiyama, K. Itaka, Y. Yamasaki, H. Koyama, K. Kataoka, *J. Am. Chem. Soc.* **2008**, *130*, 6001; b) H. Y. Wen, H. Q. Dong, W. J. Xie, Y. Y. Li, K. Wang, G. M. Paulettic, D. Shi, *Chem. Commun.* **2011**, *47*, 3550.

[18] a) H. Q. Dong, Z. L. Zhao, H. Y. Wen, Y. Y. Li, F. F. Guo, A. J. Shen, P. Frank, C. Lin, D. Shi, *Sci. China Chem.* **2010**, *53*, 2265; b) W. S. Hummers, R. E. Offeman, *J. Am. Chem. Soc.* **1958**, *80*, 1339.

[19] X. M. Sun, Z. Liu, K. Welsher, J. T. Robinson, A. Goodwin, S. Zaric, H. J. Dai, *Nano Res.* **2008**, *1*, 203.

[20] X. Y. Yang, X. Y. Zhang, Z. F. Liu, Y. F. Ma, Y. Huang, Y. S. Chen, *J. Phys. Chem. C* **2008**, *112*, 17554.

[21] L. M. Zhang, J. G. Xia, Q. H. Zhao, L. W. Liu, Z. J. Zhang, *Small* **2010**, *6*, 537.

[22] R. Cheng, F. Feng, F. H. Meng, C. Deng, J. Feijen, Z. Y. Zhong, *J. Controlled Release* **2011**, *152*, 2.

[23] a) A. N. Koo, H. J. Lee, S. E. Kim, J. H. Chang, C. Y. Park, C. Kim, J. H. Park, S. C. Lee, *Chem. Commun.* **2008**, 6570; b) L. Y. Tang, Y. C. Wang, Y. Li, J. Z. Du, J. Wang, *Bioconjugate Chem.* **2009**, *20*, 1095.

[24] a) D. A. Gewirtz, *Biochem. Pharmacol.* **1999**, *57*, 727; b) R. Hao, R. J. Xing, Z. C. Xu, Y. L. Hou, S. Gao, S. H. Sun, *Adv. Mater.* **2010**, *22*, 2729.